blood®
Regular Article

HEMATOPOIESIS AND STEM CELLS

UTX maintains the functional integrity of the murine hematopoietic system by globally regulating aging-associated genes

Yasuyuki Sera,[1,*] Yuichiro Nakata,[2,*] Takeshi Ueda,[3,*] Norimasa Yamasaki,[4] Shuhei Koide,[5] Hiroshi Kobayashi,[6] Ken-ichiro Ikeda,[4] Kohei Kobatake,[4] Masayuki Iwasaki,[1] Hideaki Oda,[7] Linda Wolff,[8] Akinori Kanai,[9] Akiko Nagamachi,[9] Toshiya Inaba,[9] Yusuke Sotomaru,[10] Tatsuo Ichinohe,[11] Miho Koizumi,[1] Yoshihiko Miyakawa,[1] Zen-ichiro Honda,[12] Atsushi Iwama,[5] Toshio Suda,[13] Keiyo Takubo,[6] and Hiroaki Honda[1]

[1]Human Disease Models, Institute of Laboratory Animals, Tokyo Women's Medical University, Tokyo, Japan; [2]Chromatin Dynamics in Stem Cells and Cancer Laboratory, Sylvester Comprehensive Cancer Center, University of Miami, Miami, FL; [3]Department of Biochemistry, Faculty of Medicine, Kindai University, Osakasayama, Japan; [4]Department of Disease Models, Research Institute for Radiation Biology and Medicine, Hiroshima University, Hiroshima, Japan; [5]Division of Stem Cell and Molecular Medicine, Center for Stem Cell Biology and Regenerative Medicine, The Institute of Medical Science, The University of Tokyo, Tokyo, Japan; [6]Department of Stem Cell Biology, Research Institute, National Center for Global Health and Medicine, Tokyo, Japan; [7]Department of Pathology, Tokyo Women's Medical University, Tokyo, Japan; [8]Laboratory of Cellular Oncology, Center for Cancer Research, National Cancer Institute, Bethesda, MD; [9]Department of Molecular Oncology, Research Institute for Radiation Biology and Medicine, [10]Natural Science Center for Basic Research and Development, and [11]Department of Hematology and Oncology, Research Institute for Radiation Biology and Medicine, Hiroshima University, Hiroshima, Japan; [12]Health Care Center and Graduate School of Humanities and Sciences, Institute of Environmental Science for Human Life, Ochanomizu University, Tokyo, Japan; and [13]Cancer Science Institute of Singapore, National University of Singapore Center for Translational Medicine, Singapore

KEY POINTS

- ***Utx* deficiency genetically compromises various metabolic and signaling pathways and phenotypically induces hematopoietic aging.**
- **UTX maintains hematopoietic stem cell function *via* both demethylase-dependent and -independent epigenetic programming.**

Epigenetic regulation is essential for the maintenance of the hematopoietic system, and its deregulation is implicated in hematopoietic disorders. In this study, UTX, a demethylase for lysine 27 on histone H3 (H3K27) and a component of COMPASS-like and SWI/SNF complexes, played an essential role in the hematopoietic system by globally regulating aging-associated genes. *Utx*-deficient ($Utx^{\Delta/\Delta}$) mice exhibited myeloid skewing with dysplasia, extramedullary hematopoiesis, impaired hematopoietic reconstituting ability, and increased susceptibility to leukemia, which are the hallmarks of hematopoietic aging. RNA-sequencing (RNA-seq) analysis revealed that *Utx* deficiency converted the gene expression profiles of young hematopoietic stem-progenitor cells (HSPCs) to those of aged HSPCs. *Utx* expression in hematopoietic stem cells declined with age, and $Utx^{\Delta/\Delta}$ HSPCs exhibited increased expression of an aging-associated marker, accumulation of reactive oxygen species, and impaired repair of DNA double-strand breaks. Pathway and chromatin immunoprecipitation analyses coupled with RNA-seq data indicated that UTX contributed to hematopoietic homeostasis mainly by maintaining the expression of genes downregulated with aging via demethylase-dependent and -independent epigenetic programming. Of note, comparison of pathway changes in $Utx^{\Delta/\Delta}$ HSPCs, aged muscle stem cells, aged fibroblasts, and aged induced neurons showed substantial overlap, strongly suggesting common aging mechanisms among different tissue stem cells. (*Blood*. 2021;137(7):908-922)

Introduction

Covalent modifications of histone tails, such as methylation, acetylation, and ubiquitination play essential roles in appropriate cell fate decisions. Trimethylated H3K27 (H3K27me3) is regarded as a repressive histone mark that functions in gene silencing.[1] H3K27 methylation is mediated by polycomb repressive complex 2 (PRC2), which comprises the catalytic subunit EZH2 and at least 2 noncatalytic subunits, EED and SUZ12.[2] On the other hand, demethylation of H3K27 is regulated by 2 distinct enzymes: ubiquitously transcribed tetratricopeptide repeat, chromosome X (UTX), also known as KDM6A, and Jumonji-C (JmjC) domain-containing protein-3 (JMJD3), also known as KDM6B,[3,4] both of which contain the JmjC domain, which exerts the demethylase activity.[3,4] However, unlike JMJD3, UTX possesses the tetratricopeptide repeat (TPR) domain that mediates protein-protein interactions and functions as a component of COMPASS (complex of proteins associated with Set 1)-like and SWI/SNF complexes.[5-8]

UTX is an X-chromosome–specific enzyme, and the male counterpart is on the Y chromosome, named ubiquitously transcribed

tetratricopeptide repeat gene, Y chromosome (UTY), also known as KDM6C.[3,4] UTX and UTY have a high structural similarity, including in the TPR and JmjC domains[4]; however, UTY possesses very low demethylase activity.[4,9] Knockout studies for UTX demonstrated that *Utx*-deficient female mice died in utero but *Utx*-deficient male mice possessing the *Uty* gene survived embryogenesis, indicating that UTY can compensate for the function of UTX during development.[10,11]

UTX contributes to various biological processes: it regulates body patterning by binding to *Hoxb1* promoter,[3,12] promotes myogenesis by demethylating muscle-specific genes,[13] determines cell fate by controlling the retinoblastoma pathway,[14] supports cardiac development during embryogenesis,[15] regulates hematopoietic cell migration,[16] plays essential roles in embryonic stem cell differentiation,[17,18] and coordinates steroid hormone-mediated autophagy.[19] In addition, UTX plays demethylase-independent roles in T-box factor–mediated gene expression, mesoderm differentiation of embryonic stem cells, and prenatal development.[8,10,20-22]

UTX dysfunction has been identified in human diseases. Somatic inactivating mutations of *Utx* were identified in various human malignancies.[23-30] In addition, functional loss of *Utx* was reported to contribute to drug resistance and disease relapse.[31,32] These findings indicated that UTX functions as a cell-fate determinant, as well as a tumor suppressor; however, its role(s) in the hematopoietic system remains to be fully understood. In this study, by generating and analyzing *Utx*-deficient mice, we found that UTX plays essential roles in the functional integrity of hematopoietic stem-progenitor cells (HSPCs) by globally regulating aging-associated genes.

Methods

Mice

The procedures for construction of the targeting vector and generation of *Utx* conditional knockout mice are described in the supplemental Information, available on the *Blood* Web site. All the animal experiments were performed in accordance with the recommendations in the Guide for the Care and Use of Laboratory Animals of Hiroshima University Animal Research Committee (permission no. 25-107) and Tokyo Women's Medical University (permission no. GE 19-066).

Statistics

Mouse survival curves were constructed by using the Kaplan–Meier methodology and compared by using the log-rank test, using GraphPad Prism software. Other statistical analyses were performed using the Student *t* test, unless otherwise stated.

A complete and detailed description of the methods is provided in the supplemental Methods.

Results

Acquired deficiency of UTX-induced abnormal hematopoietic parameters with dysplasia

To conditionally abrogate UTX function, we generated mice in which exons 11 and 12 of the *Utx* gene were flanked by 2 *loxP* sites and crossed them with tamoxifen-inducible *ERT2Cre*$^{+}$ mice (supplemental Figure 1A). *Utx* is an X-chromosome–specific gene with a male counterpart, *Uty*; hence, the results of crossing were sex dependent, producing $Utx^{flox/flox}$, *ERT2Cre*$^{+}$ females and $Utx^{flox/Uty}$, *ERT2Cre*$^{+}$ males. Quantitative polymerase chain reaction (PCR) and western blot analysis of bone marrow (BM) cells showed that, in tamoxifen-treated females, *Utx* mRNA and UTX protein were almost completely absent in $Utx^{flox/flox}$, *ERT2Cre*$^{+}$ ($Utx^{\Delta/\Delta}$) mice compared with $Utx^{flox/flox}$, *ERT2Cre*$^{-}$ ($Utx^{+/+}$) mice, whereas in tamoxifen-treated males, *Uty* messenger RNA and UTY protein were comparable in $Utx^{flox/Uty}$, *ERT2Cre*$^{-}$ ($Utx^{+/Uty}$) and $Utx^{flox/Uty}$, *ERT2Cre*$^{+}$ ($Utx^{\Delta/Uty}$) mice (supplemental Figure 1B; primer sequences for quantitative PCR are listed in supplemental Table 1). In addition, immunofluorescent staining of long-term hematopoietic stem cells (LT-HSCs) [for surface markers of hematopoietic stem-progenitor cell (HSPC) subfractions, see supplemental Table 2] of $Utx^{+/+}$, $Utx^{+/\Delta}$, and $Utx^{\Delta/\Delta}$ females and of $Utx^{+/Uty}$ and $Utx^{\Delta/Uty}$ males exhibited graded and significant increases in H3K27me3 levels, along with *Utx* deficiency, confirming that UTX functions as a demethylase for H3K27 in primitive HSCs (supplemental Figure 1C).

Then, we analyzed hematopoietic parameters in the peripheral blood (PB), BM, and spleen in $Utx^{+/+}$, $Utx^{+/\Delta}$, and $Utx^{\Delta/\Delta}$ females and also in $Utx^{+/Uty}$ and $Utx^{\Delta/Uty}$ males. Although no obvious changes were observed in $Utx^{+/+}$ and $Utx^{+/\Delta}$ mice, $Utx^{\Delta/\Delta}$ mice exhibited a significant increase in white blood cell (WBC) count, mainly of myeloid-lineage (Mac1^{+}). A significant decrease was noted in platelets in the PB (Figure 1A, top); significant increases in LT-HSCs, short-term HSCs (ST-HSCs), and Mac1^{+} cells and significant decreases in T-lineage (Thy1.2^{+}) and erythroid-lineage (Ter119^{+}) cells in the BM (Figure 1A, middle); significant increases in LSK cells (LSKs), LT-HSCs, common myeloid progenitor cells, granulocyte-monocyte progenitor cells, and Mac1^{+} cells and a significant decrease in Thy1.2^{+} cells in the spleen (Figure 1A, bottom). Compared with $Utx^{\Delta/\Delta}$ mice, the changes in $Utx^{\Delta/Uty}$ mice were less evident, showing an increase in WBC count in the PB, an increase in common myeloid progenitor cells, and a decrease in Thy1.2^{+} cells in the BM, and increases in LT-HSCs, granulocyte-monocyte progenitor cells, and Mac1^{+} cells in the spleen (supplemental Figure 2A).

In addition, morphological abnormalities were observed in $Utx^{\Delta/\Delta}$ mice (Figure 1B), which included WBCs with abnormal nuclei, including pseudo Pelger-Huët anomalies (Figure 1B1-2), neutrophils with hypersegmentation (Figure 1B3), giant platelets (Figure 1B4), erythrocytes with Howell-Jolly bodies (Figure 1B5), apoptotic cells (Figure 1B6), myeloid progenitor cells with abnormal nuclei (Figure 1B7,9-10), and micromegakaryocytes (Figure 1B8-9). These results indicate that acquired deficiency of UTX induces abnormal hematopoietic parameters with trilineage dysplasia, reminiscent of human myelodysplastic syndrome (MDS), as previously described.[16,33,34]

Extramedullary hematopoiesis in $Utx^{\Delta/\Delta}$ mice

Macroscopically, the femurs of $Utx^{\Delta/\Delta}$ mice were pale and the spleens were enlarged, compared with those of $Utx^{+/+}$ mice (supplemental Figure 3A, left). Pathological analyses revealed that the $Utx^{\Delta/\Delta}$ BM contained markedly reduced erythroid cells and megakaryocytes and the $Utx^{\Delta/\Delta}$ spleen contained an increased number of myeloid cells and megakaryocytes (supplemental Figure 3A, right). These phenotypes

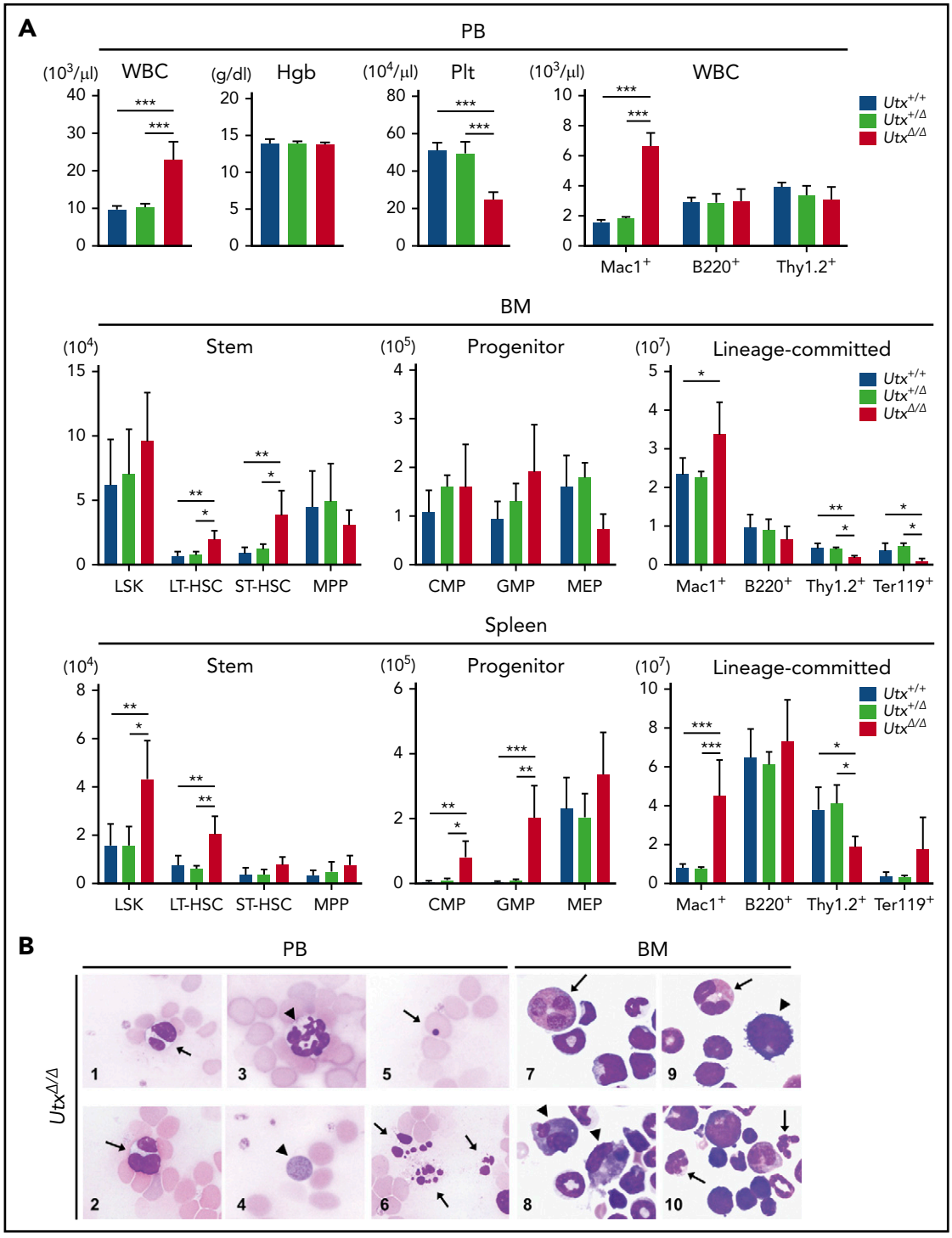

Figure 1. Analysis of hematopoietic parameters and morphological changes in *Utx*-deficient mice. (A) Analysis of hematopoietic parameters in the PB (top), BM (middle), and spleen (bottom) of $Utx^{+/+}$, $Utx^{+/\Delta}$, and $Utx^{\Delta/\Delta}$ female mice. Hgb: hemoglobin concentration, Plt: platelet number. *$P < .05$; **$P < .01$; ***$P < .001$; comparison of $Utx^{+/+}$, $Utx^{+/\Delta}$, and $Utx^{\Delta/\Delta}$ mice, assessed with a 1-way analysis of variance followed by Tukey's test. (B) Morphological changes of hematopoietic cells in the PB (panels 1-6) and BM (panels 7-10) of $Utx^{\Delta/\Delta}$ mice. WBCs with abnormal nuclei (panels 1-3), including Pseudo Pelger-Huët anomalies (arrows) and hypersegmentation (arrowhead). A giant platelet (panel 4, arrowhead). An erythrocyte with a Howell-Jolly body (panel 5, arrow). Apoptotic cells (panel 6, arrows). Myeloid progenitor cells with abnormal nuclei and micro-megakaryocytes (panels 7-10, arrows and arrowheads, respectively).

are characteristic of extramedullary hematopoiesis and suggest the transition of HSPCs from the BM to the spleen through the PB. To address this possibility, we subjected HSPCs in the PB to flow cytometry and colony formation assays. The results exhibited significant increases in c-kit$^+$ and LSK cells in the $Utx^{\Delta/\Delta}$ PB (supplemental Figure 3B), which generated a considerable number of trilineage hematopoietic cell colonies containing dysplastic cells, as observed in the $Utx^{\Delta/\Delta}$ PB and BM (supplemental Figure 3C-D), indicating circulating HSPCs in $Utx^{\Delta/\Delta}$ mice.

Impaired reconstitution ability of *Utx*$^{\Delta/\Delta}$ HSPCs

Analysis of *Utx* and *Uty* expression in HSPC subfractions showed similar patterns, being highest in the LT-HSC subfraction and decreasing as the cells differentiated (Figure 2A; supplemental Figure 2B). To investigate the repopulating ability of *Utx*$^{+/+}$ and *Utx*$^{\Delta/\Delta}$ LSKs, competitive repopulation assays were performed (Figure 2B, top). In the first bone marrow transplantation (BMT), the total PB chimerism of *Utx*$^{\Delta/\Delta}$ cells was similar to that of *Utx*$^{+/+}$ cells at 1 month, but became significantly lower at 2 and 3 months (Figure 2B, middle left). In the second BMT, the reduced PB chimerism of *Utx*$^{\Delta/\Delta}$ cells was more pronounced, and almost no contribution was detected (Figure 2B, middle right). Analysis of the lineage-positive cells in the first BMT showed that the percentage of *Utx*$^{\Delta/\Delta}$ cells was significantly reduced in all myeloid, B-cell (B220^{+}), and T-cell (Thy1.2^{+}) lineages (Figure 2B, bottom), indicating the severely impaired repopulation potential of *Utx*$^{\Delta/\Delta}$ HSPCs. We also performed a rescue experiment in which *Utx*$^{+/+}$ LSKs were transduced with an empty vector (EV) (*Utx*$^{+/+}$+EV), *Utx*$^{\Delta/\Delta}$ cells with empty vector (*Utx*$^{\Delta/\Delta}$+EV), or *Utx*$^{\Delta/\Delta}$ cells with *Utx*-expressing vector (*Utx*$^{\Delta/\Delta}$+*Utx*) were subjected to competitive reconstitution assays. Although the results were not statistically significant, *Utx*$^{\Delta/\Delta}$+*Utx* cells exhibited an enhanced engraftment capacity compared with *Utx*$^{\Delta/\Delta}$+EV cells, indicating that the impaired repopulating ability of *Utx*$^{\Delta/\Delta}$ HSPCs was a direct effect of *Utx* deficiency (Figure 2C).

The efficiency of BM reconstitution correlates strongly with the homing ability of HSPCs. Thus, we performed homing assays and also measured the expression of CXCR4, a key chemokine receptor for HSC homing.[35] Consistent with the results of a previous report,[16] *Utx*$^{\Delta/\Delta}$ LSKs exhibited a significantly reduced homing ability, despite comparable expression of *Cxcr4* (Figure 2D).

Increased leukemia susceptibility of *Utx*$^{\Delta/\Delta}$ mice

Utx is frequently mutated in human cancers[23,28] and is a tumor suppressor in mice.[33,34,36] To investigate the effect of UTX deficiency on leukemogenesis, we performed retrovirus-insertional mutagenesis using MOL4070A, a retrovirus capable of inducing leukemia.[37] *Utx*-expressing (*Utx*$^{+/+}$ and *Utx*$^{+/Uty}$) and *Utx*-deficient (*Utx*$^{\Delta/\Delta}$ and *Utx*$^{\Delta/Uty}$) mice were infected with MOL4070A as neonates, and their hematopoietic parameters were analyzed (Figure 3A, top).

During a 250-day observation period, although no disease was observed in *Utx*$^{+/+}$+MOL4070A and *Utx*$^{+/Uty}$+MOL4070A mice, all the *Utx*$^{\Delta/\Delta}$+MOL4070A and *Utx*$^{\Delta/Uty}$+MOL4070A littermates developed leukemia; the former died within 150 days and the latter within 250 days (Figure 3A, middle; supplemental Table 3). To determine the lineage of the leukemias, enlarged spleens containing infiltrating leukemic cells, were subjected to flow cytometric and gene rearrangement analyses. Leukemias were mostly acute myeloid leukemia (AML) or T-cell acute lymphoblastic leukemia (T-ALL), along with B-cell ALL in a few cases (Figure 3A, bottom; supplemental Table 3), closely corresponding to the phenotypes of human leukemias with *UTX* deficiency.[23,28]

Next, we investigated virus integration sites by inverse PCR.[37] Six common integration sites (*Sox4*, *Mecom*, *Osbpl1a*, *Notch1*, *Ikaros*, and *Tax1bp1*) were identified (supplemental Figure 4; supplemental Table 4), most of which were reported as leukemia-associated genes.[38-40] Because *Sox4* was highly expressed in tumors (supplemental Figure 4) and reported as a cooperative gene in leukemia development,[41,42] we examined the cooperative role of *Sox4* overexpression with *Utx* deficiency (Figure 3B, top). *Sox4*-expressing *Utx*$^{\Delta/\Delta}$ (*Utx*$^{\Delta/\Delta}$+*Sox4*) cells generated significantly increased colony-forming and replating abilities (Figure 3B, second row) and developed leukemia, classified as AML, at significantly higher frequency than *Sox4*-expressing *Utx*$^{+/+}$ (*Utx*$^{+/+}$+*Sox4*) cells (Figure 3B, third row and bottom left). RNA-sequencing (RNA-sea) and gene set enrichment analysis (GSEA) identified the most positively enriched pathway in *Utx*$^{\Delta/\Delta}$+*Sox4* cells as "Hedgehog signaling" (Figure 3B, bottom right), which was reported to contribute to hematopoietic malignancies.[43] *Utx* deficiency rendered hematopoietic cells susceptible to leukemia and additional gene alterations, such as *Sox4* overexpression, and promoted acute transformation, possibly through activation of aberrant signal(s).

Utx$^{\Delta/\Delta}$ LSKs exhibited the molecular signature of aged HSPCs

To clarify the molecular mechanisms underlying the *Utx* deficiency–induced hematopoietic abnormalities, we analyzed the gene expression profiles of *Utx*$^{+/+}$ and *Utx*$^{\Delta/\Delta}$ LSKs. GSEA indicated that the most positively enriched gene set in *Utx*$^{\Delta/\Delta}$ LSKs was "Oxidative phosphorylation" characterized by the upregulation of ATPases, NADH dehydrogenases, and cytochrome *c* oxidases (Figure 4A, left; supplemental Figure 5A, left; supplemental Table 5). In contrast, the most negatively enriched gene set was "TGF-β signaling," with downregulation of TGF-β receptors, Activin receptors, and Smad proteins (Figure 4A, right; supplemental Figure 5A, right; supplemental Table 5).

Notably, the phenotypes of *Utx*$^{\Delta/\Delta}$ mice, such as myeloid skewing with dysplasia, extramedullary hematopoiesis, impaired reconstitution activity, and leukemia susceptibility, are characteristics of hematopoietic aging.[44-46] In addition, upregulation of oxidative phosphorylation and downregulation of TGF-β signaling are hallmarks of an aged hematopoietic system.[47-49] Therefore, we compared the gene expression profiles of *Utx*$^{\Delta/\Delta}$ LSKs with those reported for young and aged HSPCs.[47] Interestingly, genes with enhanced expression in *Utx*$^{\Delta/\Delta}$ LSKs correlated significantly with the top 200 upregulated genes in aged HSPCs[47] (Aging Up Top200; supplemental Table 6; Figure 4B, left; supplemental Figure 5B, left). In addition, genes with reduced expression in *Utx*$^{\Delta/\Delta}$ LSKs correlated significantly with the top 200 downregulated genes in aged HSPCs[47] (Aging Down Top200; Supplemental Table 6; Figure 4B, right; supplemental Figure 5B, right). Moreover, the gene expression patterns of *Utx*$^{\Delta/\Delta}$ LSKs correlated conversely with molecular signatures of young HSPCs[50-52] (Figure 4C, top) and correlated positively with the molecular signature of myeloid cells[52] (Figure 4C, bottom). These results collectively indicate that the acquired loss of UTX converts the gene expression patterns of young HSPCs to those of aged cells.

Utx$^{\Delta/\Delta}$ HSPCs exhibited phenotypes of hematopoietic aging

We then analyzed *Utx*$^{\Delta/\Delta}$ HSPCs from the perspective of aging. We first examined changes in *Utx* expression with aging. The expression levels of *Utx* in aged (20 months) LT-HSCs, ST-HSCs, and multipotent progenitor cells decreased significantly compared with those in young (2 months) cells, confirming the

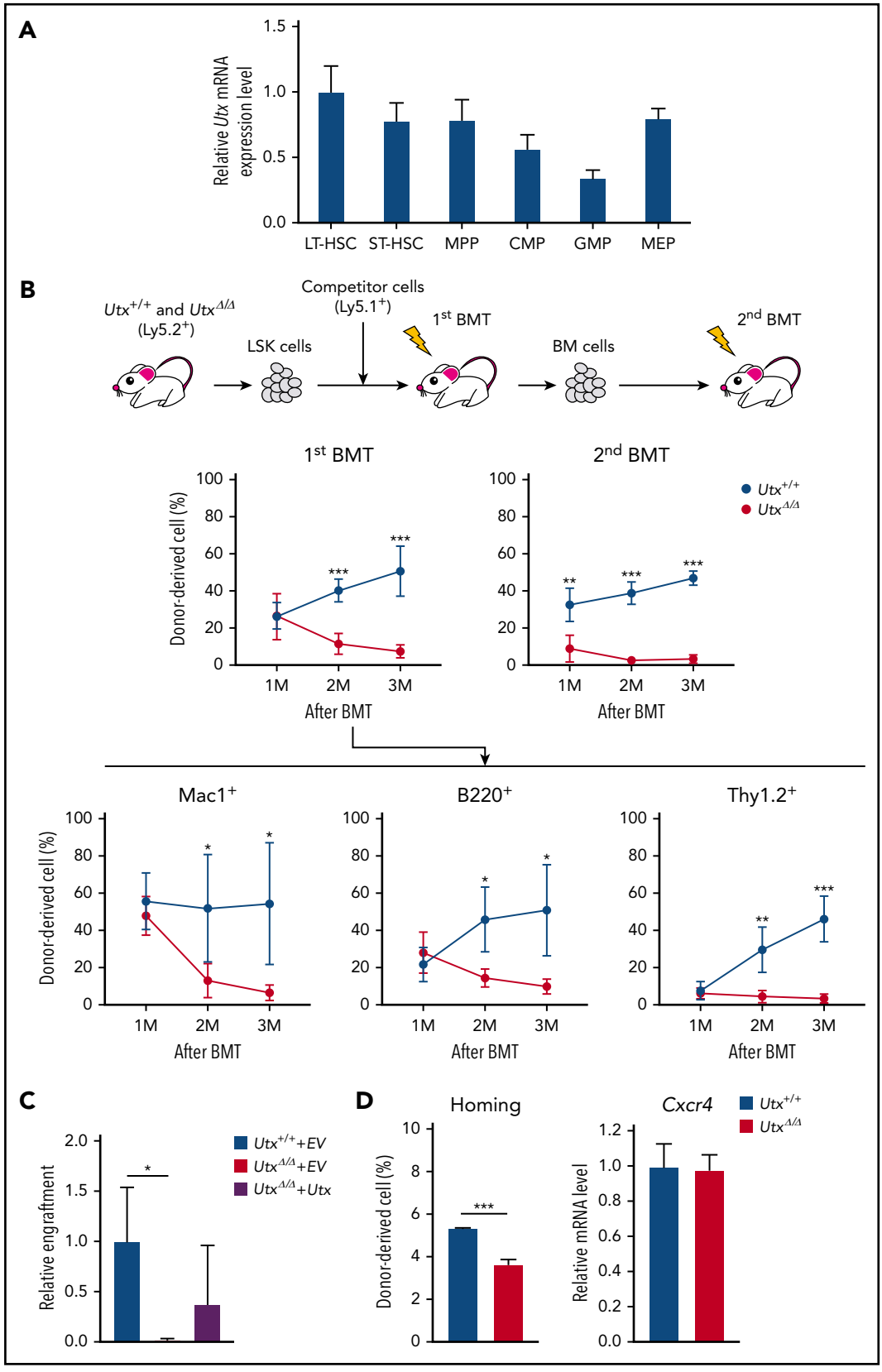

Figure 2. Expression of *Utx* in HSPCs, analysis of repopulating activity of $Utx^{\Delta/\Delta}$ HSPCs, and homing ability of $Utx^{\Delta/\Delta}$ HSPCs. (A) Relative expression levels of *Utx* in hematopoietic stem and progenitor subfractions. The results are shown relative to levels in LT-HSCs. (B) Experimental procedure for serial competitive repopulation experiments (top). Percentages of donor-derived cells in the PB of recipients of $Utx^{+/+}$ or $Utx^{\Delta/\Delta}$ cell transplants at first and second BMTs. Percentages of lineage-committed, donor-derived cells in the PB of recipients at first BMT (bottom). $^*P < .05$; $^{**}P < .01$; $^{***}P < .001$. (C) Engraftment of $Utx^{+/+}$+EV, $Utx^{\Delta/\Delta}$+EV, and $Utx^{\Delta/\Delta}$+*Utx* cells at 3 months after transplantation. The percentages of donor-derived cells in the PB are shown relative to that of $Utx^{+/+}$+EV. $^*P < .05$. (D) Homing ability (left) and expression (right) of *Cxcr4* in $Utx^{+/+}$ and $Utx^{\Delta/\Delta}$ cells. $^{***}P < .001$.

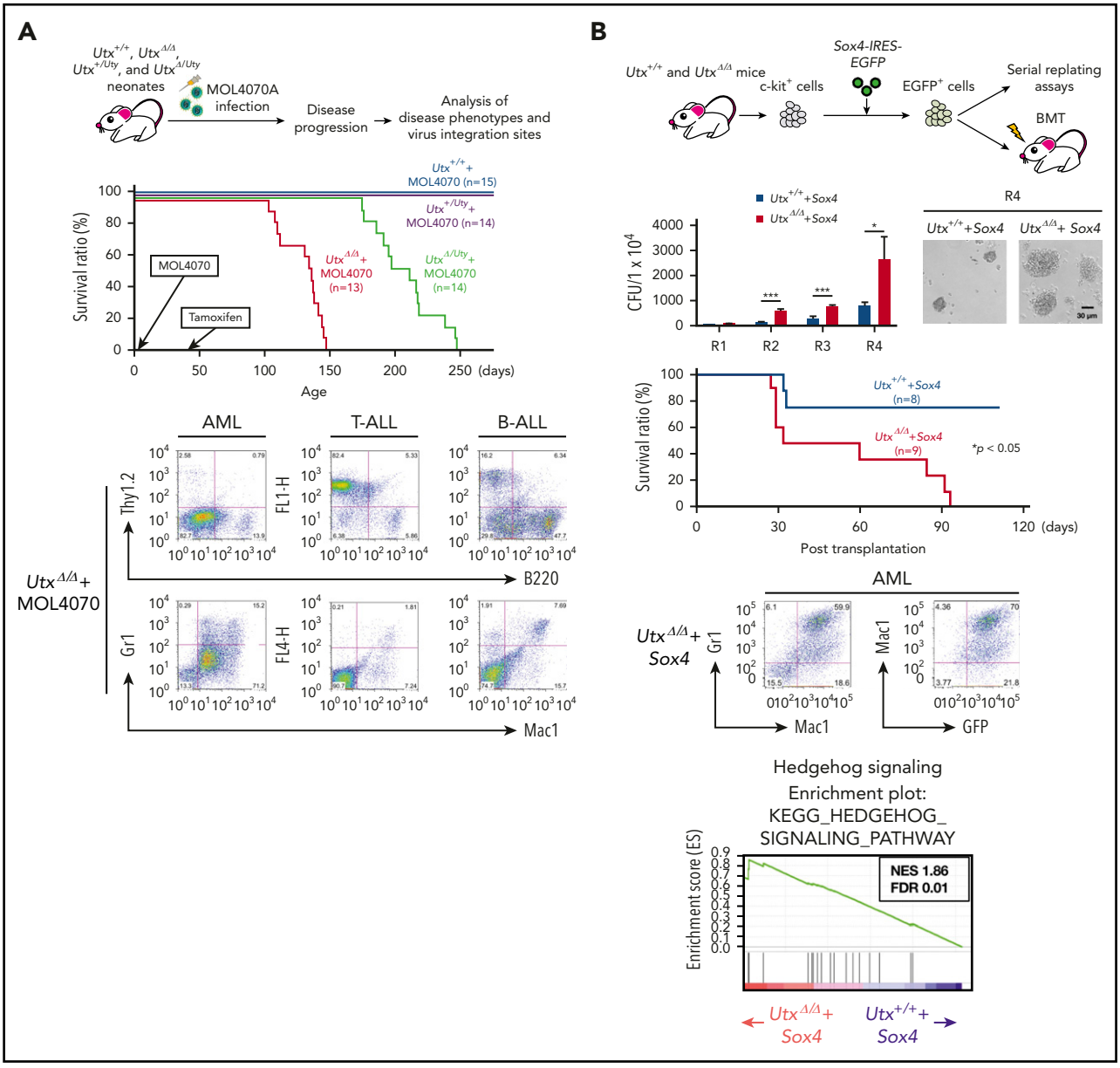

Figure 3. Analysis of leukemias developed in MOL4070A-infected *Utx*$^{\Delta/\Delta}$ and *Utx*$^{\Delta/Uty}$ mice. (A) Experimental procedure of retroviral insertional mutagenesis (top). Neonates were infected with MOL4070A, and leukemic mice were analyzed for disease phenotypes and virus integration sites (middle); survival curves are shown. Representative fluorescence-activated cell sorting results of leukemia cells (bottom), including acute myeloid leukemia (AML), T-lineage acute lymphoblastic leukemia (T-ALL), and B-lineage acute lymphoblastic leukemia (B-ALL). (B) Experimental procedure (top). c-kit$^+$ cells were transduced with *Sox4-IRES-EGFP* EV and EGFP$^+$ cells were subjected to serial replating and BMT assays and the colony-forming ability of *Utx*$^{+/+}$+*Sox4* and *Utx*$^{\Delta/\Delta}$+*Sox4* cells was observed (second row). Colony numbers at rounds 1 to 4 (R1 to R4) of replating, starting at 1×10^4 cells, and representative micrographs of colonies at R4 are shown. $^*P < .05$; $^{***}P < .001$. Survival curves of transplant recipients (third row). Representative FACS results of AML cells developed in *Utx*$^{+/+}$+*Sox4* transplant recipients (bottom left). GSEA plots of hedgehog signaling (bottom right). The plots are shown with normalized enrichment score (NES) and false discovery rate (FDR).

aging-associated decline in *Utx* expression in HSC subfractions (Figure 5A). Similarly, the expression levels of *Uty* were significantly reduced in aged HSCs (supplemental Figure 2C).

A previous study reported that the expression of CD41, a megakaryocyte/platelet marker, increases with age.[53] After confirming that aged (18 months) LSK-gated c-kit$^+$ cells expressed CD41 at a high level, we measured CD41 expression in young (2 months) *Utx*$^{+/+}$ and *Utx*$^{\Delta/\Delta}$ cells and found that *Utx*$^{\Delta/\Delta}$ cells expressed CD41 at a significantly higher level than *Utx*$^{+/+}$ cells (Figure 5B). In addition, the marked enrichment of the oxidative phosphorylation in *Utx*$^{\Delta/\Delta}$ LSKs (Figure 4A, left) strongly suggested an increase in reactive oxygen species (ROS), which is implicated in the aging process.[49] In fact, measurement of ROS in *Utx*$^{+/+}$ and *Utx*$^{\Delta/\Delta}$ LSKs and LT-HSCs demonstrated a significant accumulation of ROS in *Utx*$^{\Delta/\Delta}$ cells (Figure 5C). We also found positive enrichment of glutathione metabolism pathway in *Utx*$^{\Delta/\Delta}$ cells (supplemental Figure 6A), which would be activated to scavenge the accumulated ROS. Another aspect of aged HSPCs is impaired recovery from the DNA damage response (DDR).[54,55] The analysis of the behavior and localization of DNA repair proteins in irradiated *Utx*$^{+/+}$ and *Utx*$^{\Delta/\Delta}$ LT-HSCs showed

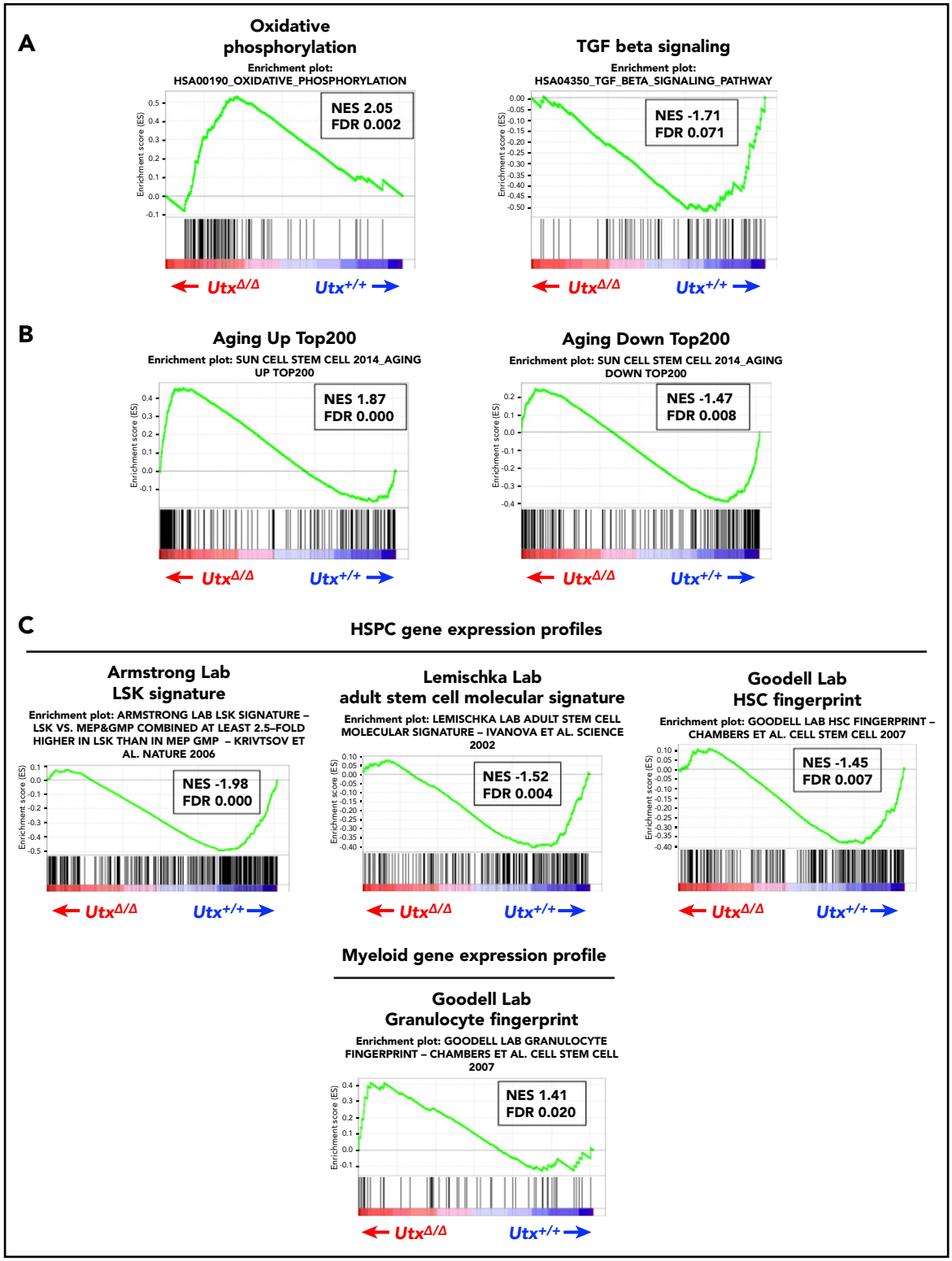

Figure 4. GSEA of RNA expression profiles of *Utx*$^{\Delta/\Delta}$ LSKs. (A) GSEA plots of *Utx*$^{\Delta/\Delta}$ vs *Utx*$^{+/+}$ LSKs. The results of the most positively enriched plot (Oxidative phosphorylation) and most negatively depleted plot (TGF beta signaling) in *Utx*$^{\Delta/\Delta}$ LSKs are shown with normalized enrichment score (NES) and false discovery rate (FDR). (B) GSEA plots comparing differently expressed genes in *Utx*$^{\Delta/\Delta}$ and *Utx*$^{+/+}$ LSKs and aging-associated genes in HSPCs.[47] The results of plots that increased with age (Aging Up Top200) and decreased with age (Aging Down Top200) are shown with NES and FDR. (C) GSEA plots comparing *Utx*$^{\Delta/\Delta}$ LSK genes with HSPC and myeloid gene signatures. The results of comparison with 3 HSPC expression profiles (Armstrong Laboratory, Lemischka Laboratory, and Goodell Laboratory)[50-52] and with a myeloid expression profile (Goodell Laboratory)[52] are shown with NES and FDR.

Figure 5. Analysis of aging-associated phenotypes in *Utx*$^{\Delta/\Delta}$ HSPCs. (A) Expression changes of *Utx* in young (2 months [M]) and aged (20 months) HSC subfractions. The results are shown relative to that in LT-HSCs. *$P < .05$. (B) Expression of CD41, an aging-related marker, in LSK-gated c-kit$^+$ cells of aged (18 months) wild-type (*WT*) and young (2 months) *Utx*$^{+/+}$ and *Utx*$^{\Delta/\Delta}$ mice. Representative results of fluorescence-activated cell sorting and a comparison of percentages of CD41$^+$, LSK-gated c-kit$^+$ cells in young *Utx*$^{+/+}$ and *Utx*$^{\Delta/\Delta}$ mice are shown. **$P < .01$. (C) ROS levels in LSKs and LT-HSCs of *Utx*$^{+/+}$ and *Utx*$^{\Delta/\Delta}$ mice. The representative histograms and fluorescence intensities are shown. **$P < .01$; ***$P < .001$. (D) Kinetics of DDR in *Utx*$^{+/+}$ and *Utx*$^{\Delta/\Delta}$ LT-HSCs (0, 3, 18, and 24 hours) after 2 Gy of irradiation. Representative images of γH2AX (green) and 53BP1 (red) foci (top) and the number of γH2AX/53BP1-overlapping foci (bottom) in cells are shown, respectively. Residual γH2AX and 53BP1 foci in *Utx*$^{\Delta/\Delta}$ cells at 18 hours after irradiation (arrow). **$P < .01$.

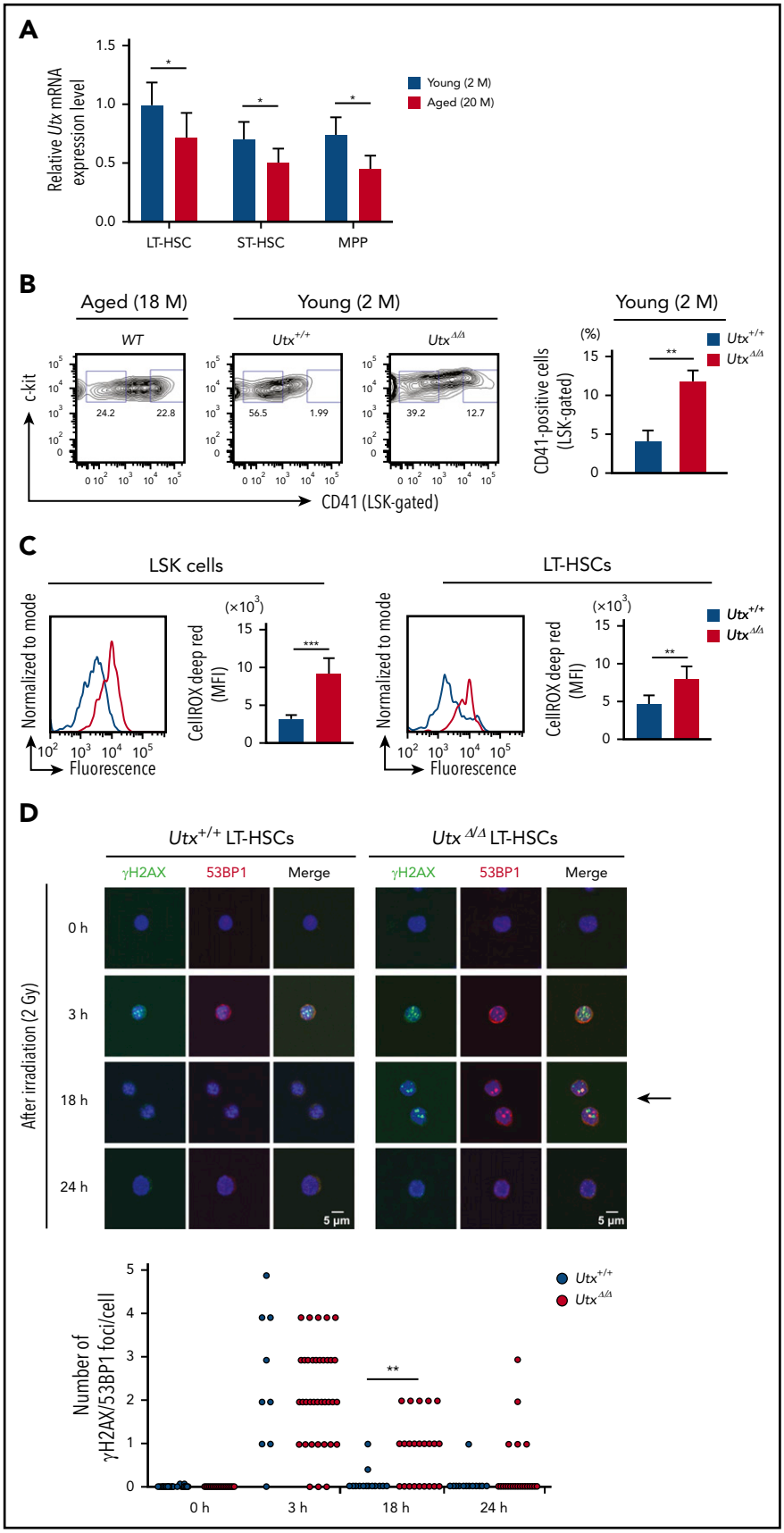

that, although a similar number of γH2AX/53BP1-overlapping foci developed at 2 hours and finally cleared by 24 hours, $Utx^{\Delta/\Delta}$ LT-HSCs exhibited significantly delayed repair kinetics and DDR remnants at 18 hours (Figure 5D). Because expression levels of DDR-associated genes were comparable between $Utx^{+/+}$ and $Utx^{\Delta/\Delta}$ LSKs, although there was a slight decrease in *Xrcc5* in $Utx^{\Delta/\Delta}$ cells after irradiation[56,57] (supplemental Figure 6B), this phenotype may be related to *Utx* deficiency–induced altered chromatin accessibility at the DNA damage sites, as reported in a previous study.[34]

Introduction of *Utx* in aged HSPCs partly restored the impaired repopulating activity and reversed the expression of aging-associated genes

We investigated whether the reexpression of *Utx* can rescue the functional defects of aged HSPCs in terms of reconstitution ability. To examine the contribution of the demethylase activity of UTX, we transduced aged (20 months) LSKs with EV-, wild-type *Utx* (Utx^{WT})-, or demethylase-dead *Utx* (Utx^{DD})[10]-*IRES-EGFP* vector (referred to as EV-, Utx^{WT}-, or Utx^{DD}-*IRES-EGFP*), and c-kit$^+$, EGFP$^+$ cells were subjected to competitive repopulation assays (Figure 6A, top). Whereas all transplant-recipient mice receiving EV-*IRES-EGFP*–transduced or Utx^{DD}-*IRES-EGFP*–transduced aged LSKs (Aged+EV and Aged+Utx^{DD}) exhibited failed reconstitution (<1% PB chimerism),[58] several recipients transplanted with Utx^{WT}-*IRES-EGFP*-transduced aged cells (Aged+Utx^{WT}) were successfully reconstituted (>1% PB chimerism)[58] (reconstituted mice numbered 1-3; Figure 6A, bottom left). Interestingly, the degree of reconstitution correlated well with increased levels of *Utx* expression and decreased myeloid-biased differentiation (Figure 6A, bottom right). In addition, we found that the enforced *Utx* expression in aged cells significantly reduced the H3K27me3 levels and also significantly reversed the expression of P-selectin (*Selp*) and clusterin (*Clu*), the hallmark genes of hematopoietic aging (Figure 6B).[52] These findings indicate that *Utx* restores the aging-related phenotypes, at least in part, through reprogramming the H3K27 methylation status.

UTX regulates aging-associated genes via demethylase-dependent and -independent mechanisms

To analyze aging-associated genes regulated by UTX-mediated demethylation, $Utx^{+/+}$ and $Utx^{\Delta/\Delta}$ LSKs were subjected to chromatin immunoprecipitation sequencing (ChIP-seq) for H3K27me3. The number of H3K27me3 peaks was higher in $Utx^{\Delta/\Delta}$ LSKs than in $Utx^{+/+}$ LSKs (Figure 7A). The genomic regions with H3K27me3 peaks in $Utx^{\Delta/\Delta}$ LSKs were subjected to the biological processes of DNA binding and transcriptional regulation in gene ontology enrichment analysis (Figure 7B). Of note, motif and pathway analyses revealed that the regions with H3K27me3 peaks in $Utx^{\Delta/\Delta}$ LSKs were significantly enriched in the expected binding sites of SMAD, SP1, and EGR1, which are downstream transcription factors of TGF-β and are expected to functionally decline during aging[47,48] (Figure 7C-D). To investigate the direct regulation of UTX at TGF-β signaling-associated gene loci, we searched for genes with decreased expression and increased H3K27me3 levels around the transcription start site (TSS) ± 5 kb. The results identified *Hnf4a* and *Col1a1*, which are TGF-β signaling-associated genes[59,60] and are included in Aging Down Top200,[47] suggesting that these are direct targets of UTX (Figure 7E).

UTX regulates gene expression in a demethylase-independent manner as a component of COMPASS-like and SWI/SNF complexes.[5-8] To analyze demethylase-independent roles of UTX in the expression of aging-associated genes, we picked up commonly upregulated and downregulated genes between RNA-seq data of $Utx^{\Delta/\Delta}$ LSKs and Aging Up/Down Top200 (Figure 7F, named Up genes and Down genes, respectively) and searched for the binding of KMT2D and BRG1/SMARCA4, the key components of COMPASS-like and SWI/SNF complexes, respectively, to the regulatory regions (TSS ± 5 kb) of the genes, by referring to published data sets.[61-68] We found KMT2D peaks only in Down genes (~20%; Figure 7G). In addition, although SMARCA4 binds to both Up and Down genes, the total peak number was much higher in Down genes than in Up genes (430 vs 132) and co-occupancy of KMT2D and SMARCA4 was observed in 13 genes (Figure 7H). These results collectively suggest that UTX mainly regulates the expression of genes downregulated with aging, through both demethylase-dependent and -independent mechanisms.

Discussion

There has been increasing interest in how stem cells maintain tissue homeostasis and in how their dysfunctions induce aging.[69,70] Epigenetic deregulation has been reported to contribute to the aging process of HSPCs.[71,72] For example, deletion of sirtuin (*Sirt*) family genes encoding histone deacetylases, such as *Sirt1*, *Sirt3*, *Sirt6*, and *Sirt7*, was reported to induce hematopoietic aging through accumulating DNA damage, reduced resistance to oxidative stress, aberrant activation of WNT signaling, and impaired mitochondrial biogenesis.[73-77] Deregulation of histone methylation is also deeply implicated in aging[47,78]; however, the underlying molecular mechanisms remain less understood.

In this study, we demonstrated that deficiency of UTX, a demethylase for H3K27 and a component of the COMPASS-like and SWI/SNF complexes, induces phenotypes characteristic of hematopoietic aging. $Utx^{\Delta/\Delta}$ mice exhibited abnormal hematopoietic differentiation with myeloid skewing, MDS-like morphological changes, extramedullary hematopoiesis, impaired repopulation ability, and high susceptibility to leukemia (Figures 1-3). RNA-seq analysis revealed that *Utx* deficiency converted the gene expression profiles of young HSPCs to those of aged cells (Figure 4). The expression levels of *Utx* in HSCs decline with age, and $Utx^{\Delta/\Delta}$ HSPCs exhibited an increase in the expression of an aging-associated marker, accumulation of ROS, and impaired DDR after irradiation (Figure 5). These findings collectively indicate that *Utx* deficiency genetically compromises various metabolic and signaling pathways and phenotypically induces hematopoietic aging.

It remains controversial whether UTX functions as an oncogene or antioncogene.[79] In T-ALL cases, a previous report showed that UTX acts as an oncogene in TAL1-driven T-ALL.[80] In contrast, we and others[36,81] have provided evidence that UTX functions as an antioncogene in T-ALL. The results seem contradictory. However, interestingly, in the report by Van der Meulen et al,[81] all the T-ALL cases with *UTX* mutations were associated with *TLX3* and/or *NOTCH1* mutations, and none of them cooccurred with *TAL1* mutations. In addition, in our mutagenesis study, *Tal1* was not detected as a cooperative gene (supplemental Table 4). Thus,

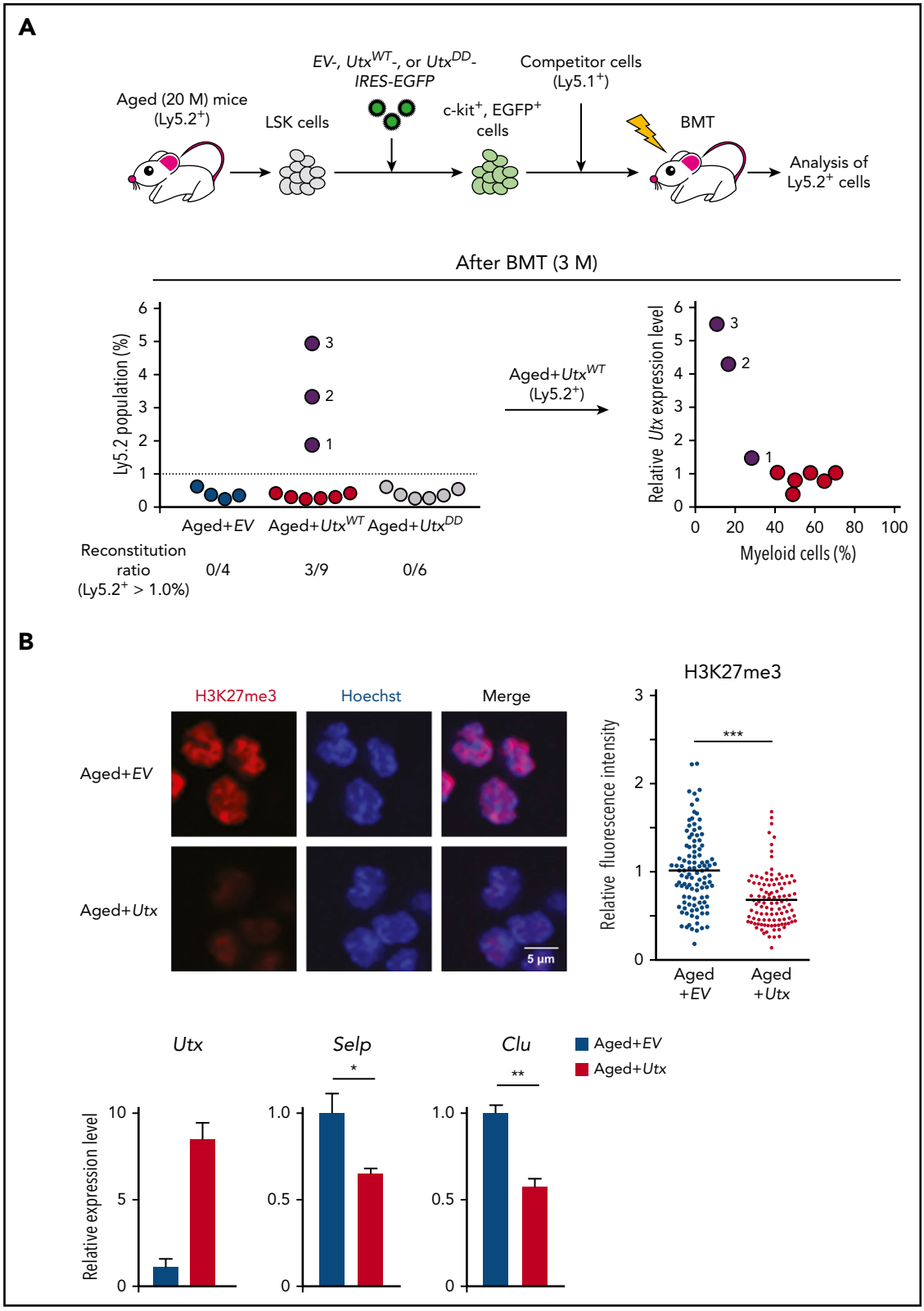

Figure 6. Partial restoration of impaired reconstitution ability of aged HSPCs and expression changes of aging-associated genes by reexpression of *Utx*. (A) Reexpression of *Utx* in aged HSPCs and the results of reconstitution. Experimental procedure (top). Aged (20 months [M]) LSKs were transduced with empty vector (EV)-, wild-type *Utx* (Utx^{WT})-, or demethylase-dead *Utx* (Utx^{DD})-*IRES-EGFP* and c-kit$^+$, EGFP$^+$ cells were subjected to competitive repopulation assays. The PB chimerisms of Aged+EV, Aged+Utx^{WT}, or Aged+Utx^{DD} cell transplant recipients at 3 months after transplantation (bottom left). The successfully reconstituted Aged+Utx^{WT} cell (Ly5.2$^+$ >1.0%) transplant recipients are numbered. Correlation between relative *Utx* expression levels in Ly5.2$^+$ BM cells and percentages of myeloid cells in Ly5.2$^+$ PB cells in Aged+Utx^{WT} cell recipients (bottom right). The numbered mice are the same in both panels. (B) Changes in H3K27me3 expression (top; ***$P < .001$) and levels of selectin P (*SelP*) and clusterin (*Clu*) in Aged+EV and Aged+*Utx* c-kit$^+$, EGFP$^+$ cells (bottom). *$P < .05$; **$P < .01$.

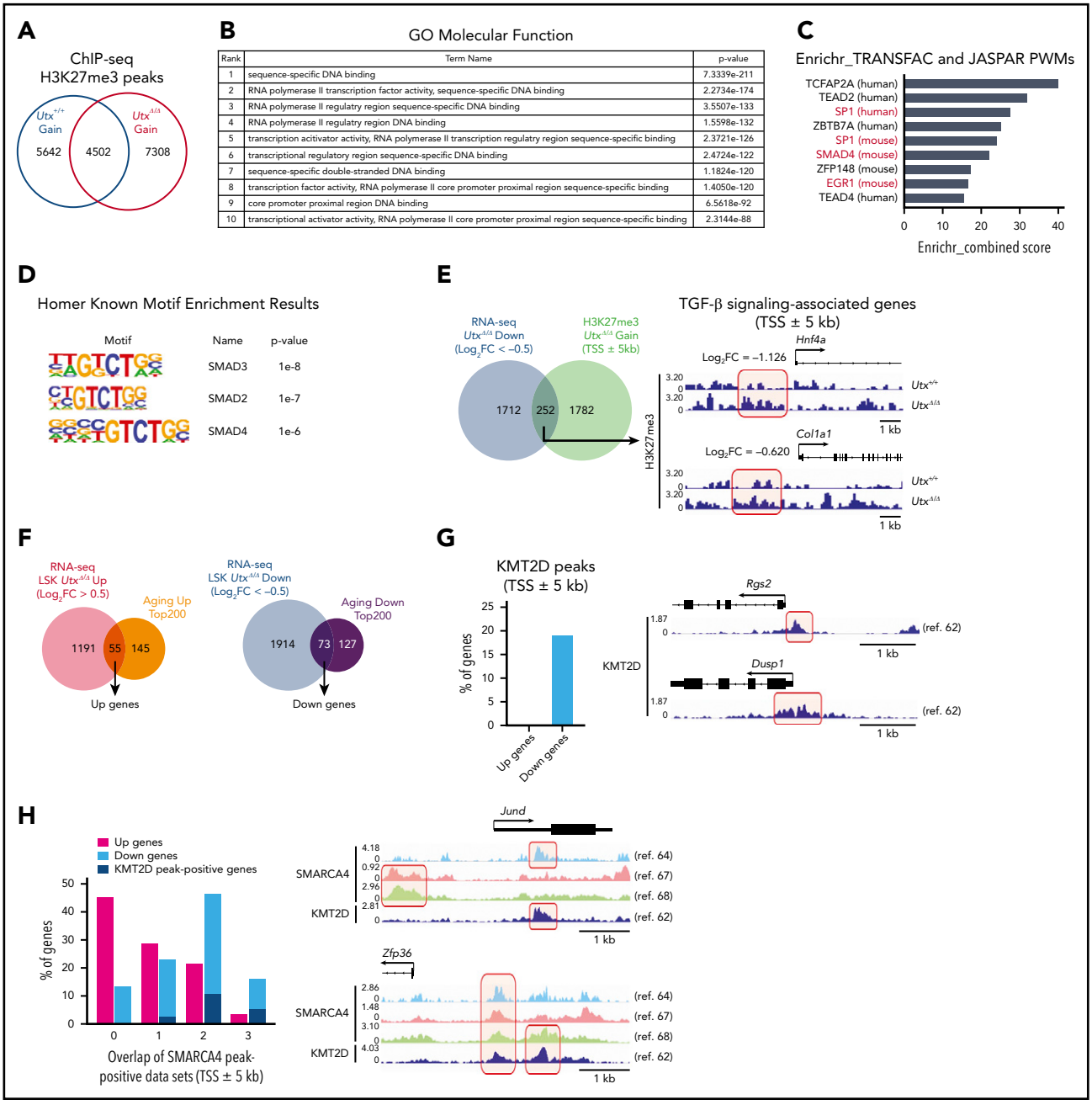

Figure 7. Results of ChIP-seq analysis for H3K27me3, KMT2D, and SMARCA4. (A) Venn diagram showing the overlap of statistically significant peaks of H3K27me3 between *Utx*$^{+/+}$ and *Utx*$^{\Delta/\Delta}$ LSKs. (B) Gene ontology (GO) enrichment analysis of the genes with H3K27me3 peaks in *Utx*$^{\Delta/\Delta}$ LSKs with the Genomic Regions Enrichment of Annotations Tool (GREAT). The ranks were calculated by *P* values. (C) Pathway analysis of the genomic regions with H3K27me3 peaks in *Utx*$^{\Delta/\Delta}$ LSKs with Enrichr_TRANSFAC and JASPAR position weight matrice (PWM) databases. TGF-β downstream transcription factors are shown in red. (D) SMAD proteins SMAD3, SMAD2, and SMAD4, detected from transcription factor motif analysis of the genomic regions with H3K27me3 peaks in *Utx*$^{\Delta/\Delta}$ LSKs with Homer Known Motif Enrichment Results. (E) Venn diagram (left) showing the overlap between genes downregulated ($Log_2FC < -0.5$) by *Utx* deficiency and those with elevated H3K27me3 peaks around annotated TSS ± 5 kb by *Utx* deficiency. The overlay of H3K27me3 peaks at the representative TGF-β signaling-associated gene loci (right), *Hnf4a* and *Col1a1*, in *Utx*$^{+/+}$ and *Utx*$^{\Delta/\Delta}$ LSKs. Remarkable H3K27me3 peaks in *Utx*$^{\Delta/\Delta}$ LSKs are outlined in red. (F) Venn diagrams showing the overlap between upregulated ($Log_2FC > 0.5$) genes in *Utx*$^{\Delta/\Delta}$ LSKs and Aging Up Top200 (Up genes, left) and the overlap between downregulated ($Log_2FC < -0.5$) genes in *Utx*$^{\Delta/\Delta}$ LSKs and Aging Down Top200 (Down genes, right). (G) Bar graph (left) showing the percentage of KMT2D binding (TSS ± 5 kb) of Up and Down genes in at least 1 of the published ChIP-seq data sets of mouse blood tissues available in the ChIP Atlas,[61] GSE69162,[62] and GSE 103508.[62] The bigwig files and bed files were obtained from the ChIP Atlas. The significance threshold for significant peaks is defined as $q < 1 \times 10^{-10}$. Overlay of KMT2D peaks at the indicated Down gene loci as representative images (right). Remarkable KMT2D peaks are outlined in red. (H) Histogram (left) showing the percentage of genes bound to SMARCA4 (TSS ± 5 kb) in Up or Down genes in at least 1 of the published ChIP-seq data sets of mouse blood tissues available in ChIP-Atlas,[61] GSE23719,[64] GSE79391,[64] GSE82144,[68] GSE52279,[65] and GSE66978.[66] The bigwig files and bed files were obtained from the ChIP-Atlas. Significance threshold for significant peaks is defined as $q < 1 \times 10^{-10}$. The columns indicate the percentages of Up genes, Down genes, KMT2D peak-positive genes with SMARCA4 peaks, respectively. The number of the horizontal axis shows the overlap of SMARCA4 peaks from different data sets. The overlay of SMARCA4 and KMT2D peaks (TSS ± 5 kb) at the indicated Down genes loci in which SMARCA4 peaks were observed in 3 data sets and a KMT2D peak was overlapped with ≥1 SMARCA4 peaks (right).

whether UTX functions as an oncogene or antioncogene may depend on the driver mutation, and its tumorigenic role may vary in different cellular contexts.

It remains to be clarified whether UTX maintains the functional integrity of HSPCs via demethylase-dependent and/or -independent mechanisms. H3K27me3 staining of *Utx*$^{+/+}$ and *Utx*$^{\Delta/\Delta}$ LT-HSCs showed graded and significant increases in H3K27me3 levels, along with *Utx*-deficiency (supplemental Figure 1C). In addition, in our experimental system, demethylase-dead *Utx* did not rescue the aged phenotype (Figure 6A). Moreover, motif and pathway analyses of the H3K27me3 ChIP data identified transcription factors involved in TGF-β signaling (Figures 7C-D), the most downregulated pathway in *Utx*$^{\Delta/\Delta}$ HSPCs (Figure 4A). These data support demethylase-dependent mechanisms. However, the overlap between promoter regions with gains of H3K27me3 by *Utx* deficiency and Aging Down Top200 was found in a small subset (Figure 7E). In addition, comparison of RNA-seq data of HSPCs deficient in *Ezh2*, encoding an H3K27 methyltransferase of PRC2,[82,83] with those of our *Utx*$^{\Delta/\Delta}$ HSPCs showed that EZH2 targets were classified into 2 groups that would represent methylation-dependent and -independent genes (supplemental Figure 7A). Moreover, comparison of the same data with Aging Up/Down Top200 exhibited much less enrichment than *Utx*$^{\Delta/\Delta}$ HSPCs (supplemental Figure 7B). These findings suggest that there are demethylase-independent mechanism(s). Indeed, the search for binding of KMT2D and SMARCA4, the key components of COMPASS-like and SWI/SNF complexes, to the regulatory region of aging-associated genes revealed that KMT2D selectively and SMARCA4 preferentially bind to Down genes with frequent co-occupancy (Figure 7F-H). These results collectively suggest that UTX contributes to hematopoietic homeostasis, mainly by maintaining the expression of genes downregulated with aging, through both demethylase-dependent and -independent epigenetic programming. The upregulation of oxidative phosphorylation (Figure 4A) may be a secondary effect, because previous studies demonstrated that TGF-β signaling suppresses oxidative phosphorylation.[84,85]

Whether stem cell aging undergoes similar genetic and/or epigenetic pathways in the different tissues is an intriguing question. An increase in H3K27me3 levels at the transcription start sites was reported, not only in aged HSPCs but also in muscle stem cells (MSCs),[86] suggesting that the functional decline of UTX contributes to MSC aging as well as HSC aging. This idea is supported by a study reporting that UTX promotes MSC regeneration through the demethylation of H3K27me3.[87] Therefore, we compared changes in signaling pathways between *Utx*$^{\Delta/\Delta}$ LSKs and aged MSCs.[88] Interestingly, we found a substantial overlap between positively and negatively enriched pathways. In upregulated pathways, 10 of 17 positively enriched pathways of aged MSCs[88] overlapped with the top 50 positively enriched pathways of *Utx*$^{\Delta/\Delta}$ LSKs, and in downregulated pathways, 26 of the top 50 negatively enriched pathways of aged MSCs[88] overlapped with the top 50 negatively enriched pathways of *Utx*$^{\Delta/\Delta}$ LSKs (supplemental Figure 8; see also supplemental Tables 5 and 7). Moreover, we compared the changed pathways not only in aged MSCs but also in aged fibroblasts and aged induced neurons (iNs)[89] to those in *Utx*$^{\Delta/\Delta}$ LSKs. We found that all of the statistically significantly enriched pathways in aged fibroblasts and aged iNs[89] were included in the top 30 significantly downregulated pathways in *Utx*$^{\Delta/\Delta}$ LSKs (supplemental Figure 9), strongly suggesting that the deregulation of specific sets of pathways may underlie stem cell aging in different tissues. Of note, the statistical change of calcium pathway was commonly observed in all the cell types examined (indicated by an asterisk in supplemental Figure 9), suggesting that this pathway is pivotal in maintaining the homeostasis of different stem cells, as suggested in previous studies.[90,91]

Interestingly, although only minimal changes were observed in the hematopoietic parameters of *Utx*$^{\Delta/Uty}$ males (supplemental Figure 2), retroviral insertional mutagenesis induced leukemia in *Utx*$^{\Delta/Uty}$ males (Figure 3A). Our findings, together with the results of previous studies,[10,11,16,81] indicate that UTY compensates for the absence of UTX in steady-state hematopoiesis but cannot compensate for UTX function as a tumor suppressor. UTY exerts very low demethylase activity but possesses the TPR domain[4,9]; hence, it is intriguing to clarify the compensatory roles of UTY for UTX deficiency in different physiological and pathological conditions.[34,92,93]

In summary, our findings demonstrate that UTX plays a pivotal role in the functional integrity of HSPCs and maintenance of hematopoietic homeostasis by globally regulating aging-associated genes. Further studies are necessary to clarify how UTX recognizes aging-related genes and whether the enhanced expression of UTX can prevent aging.

Acknowledgments

The authors thank Yuki Sakai, Sawako Ogata, Rika Tai, and Yoshio Mitamura for providing animal care, genotyping, and performing molecular experiments and Junji Takeda and the RIKEN BioResource Center for providing KY1.1 ES cells and B6-Tg(CAG-FLPe)36 mice (RBRC01834), respectively.

This work was supported by Japanese Society for the Promotion of Science (JSPS) KAKENHI grant 17J05696 (Y. Sera) and grants 19H03693 and 19K22546 (H.H.); a research grant from The Japanese Society of Hematology (Y. Sera); and funding from the Medical Research Institute (MRI), Tokyo Women's Medical University.

Authorship

Contribution: Y. Sera, Y.N., T.U., T. Inaba, Y. Sotomaru, T. Ichinohe., M.K., Y.M., Z.-i.H., T.S., K.T. and H.H. designed the research, generated the genetically engineered mice, and wrote the manuscript; Y. Sera, Y.N., T.U., N.Y., H.K., K.-i.I., K.K., M.I., A.N., and K.T. performed hematopoietic cell analyses; A.K. analyzed the RNA-seq data; S.K. and A.I. analyzed the ChIP data; H.O. examined pathological specimens; L.W. generated the MOL4070A retrovirus; and all authors reviewed and agreed on the final version of the manuscript.

Conflict-of-interest disclosure: The authors declare no competing financial interests.

ORCID profiles: T. Inaba, 0000-0002-3455-6010; T. Ichinohe, 0000-0002-0393-4066.

Correspondence: Hiroaki Honda. Institute of Laboratory Animals, Tokyo Women's Medical University, 8-1 Kawada-cho, Shinjuku-ku, Tokyo 162-8666, Japan; e-mail: honda.hiroaki@twmu.ac.jp.

Footnotes

Submitted 8 April 2019; accepted 18 September 2020; prepublished online on *Blood* First Edition 10 November 2020. DOI 10.1182/blood.2019001044.

*Y.S., Y.N., and T.U. contributed equally to this study.

The RNA-seq and ChIP-seq data obtained in this study have been deposited in the DNA Data Bank of Japan (DDBJ) and BioSample (accession numbers DRX046253 and DRX046254 for RNA-seq for $Utx^{+/+}$ and $Utx^{\Delta/\Delta}$ LSKs and accession numbers DRA010250 for $Utx^{+/+}$+*Sox4* and $Utx^{\Delta/\Delta}$+*Sox4* cells and DRA010152 for ChIP-seq for H3K27me3).

Original data are available by e-mail request to the corresponding author (honda.hiroaki@twmu.ac.jp).

The online version of this article contains a data supplement.

The publication costs of this article were defrayed in part by page charge payment. Therefore, and solely to indicate this fact, this article is hereby marked "advertisement" in accordance with 18 USC section 1734.

REFERENCES

1. Simon JA, Kingston RE. Mechanisms of polycomb gene silencing: knowns and unknowns. *Nat Rev Mol Cell Biol*. 2009;10(10):697-708.
2. Conway E, Healy E, Bracken AP. PRC2 mediated H3K27 methylations in cellular identity and cancer. *Curr Opin Cell Biol*. 2015;37:42-48.
3. Agger K, Cloos PA, Christensen J, et al. UTX and JMJD3 are histone H3K27 demethylases involved in HOX gene regulation and development. *Nature*. 2007;449(7163):731-734.
4. Hong S, Cho YW, Yu LR, Yu H, Veenstra TD, Ge K. Identification of JmjC domain-containing UTX and JMJD3 as histone H3 lysine 27 demethylases. *Proc Natl Acad Sci USA*. 2007;104(47):18439-18444.
5. Ford DJ, Dingwall AK. The cancer COMPASS: navigating the functions of MLL complexes in cancer [published correction appears in *Cancer Genet*. 2019;233-234:102]. *Cancer Genet*. 2015;208(5):178-191.
6. Shilatifard A. The COMPASS family of histone H3K4 methylases: mechanisms of regulation in development and disease pathogenesis. *Annu Rev Biochem*. 2012;81(1):65-95.
7. Van der Meulen J, Speleman F, Van Vlierberghe P. The H3K27me3 demethylase UTX in normal development and disease. *Epigenetics*. 2014;9(5):658-668.
8. Miller SA, Mohn SE, Weinmann AS. Jmjd3 and UTX play a demethylase-independent role in chromatin remodeling to regulate T-box family member-dependent gene expression. *Mol Cell*. 2010;40(4):594-605.
9. Walport LJ, Hopkinson RJ, Vollmar M, et al. Human UTY(KDM6C) is a male-specific Nε-methyl lysyl demethylase. *J Biol Chem*. 2014;289(26):18302-18313.
10. Wang C, Lee JE, Cho YW, et al. UTX regulates mesoderm differentiation of embryonic stem cells independent of H3K27 demethylase activity. *Proc Natl Acad Sci USA*. 2012;109(38):15324-15329.
11. Welstead GG, Creyghton MP, Bilodeau S, et al. X-linked H3K27me3 demethylase Utx is required for embryonic development in a sex-specific manner. *Proc Natl Acad Sci USA*. 2012;109(32):13004-13009.
12. Lee MG, Villa R, Trojer P, et al. Demethylation of H3K27 regulates polycomb recruitment and H2A ubiquitination. *Science*. 2007;318(5849):447-450.
13. Seenundun S, Rampalli S, Liu QC, et al. UTX mediates demethylation of H3K27me3 at muscle-specific genes during myogenesis. *EMBO J*. 2010;29(8):1401-1411.
14. Wang JK, Tsai MC, Poulin G, et al. The histone demethylase UTX enables RB-dependent cell fate control. *Genes Dev*. 2010;24(4):327-332.
15. Lee S, Lee JW, Lee SK. UTX, a histone H3-lysine 27 demethylase, acts as a critical switch to activate the cardiac developmental program. *Dev Cell*. 2012;22(1):25-37.
16. Thieme S, Gyárfás T, Richter C, et al. The histone demethylase UTX regulates stem cell migration and hematopoiesis. *Blood*. 2013;121(13):2462-2473.
17. Jiang W, Wang J, Zhang Y. Histone H3K27me3 demethylases KDM6A and KDM6B modulate definitive endoderm differentiation from human ESCs by regulating WNT signaling pathway. *Cell Res*. 2013;23(1):122-130.
18. Morales Torres C, Laugesen A, Helin K. Utx is required for proper induction of ectoderm and mesoderm during differentiation of embryonic stem cells. *PLoS One*. 2013;8(4):e60020.
19. Denton D, Aung-Htut MT, Lorensuhewa N, et al. UTX coordinates steroid hormone-mediated autophagy and cell death. *Nat Commun*. 2013;4(1):2916.
20. Shpargel KB, Sengoku T, Yokoyama S, Magnuson T. UTX and UTY demonstrate histone demethylase-independent function in mouse embryonic development. *PLoS Genet*. 2012;8(9):e1002964.
21. Vandamme J, Lettier G, Sidoli S, Di Schiavi E, Nørregaard Jensen O, Salcini AE. The C. elegans H3K27 demethylase UTX-1 is essential for normal development, independent of its enzymatic activity. *PLoS Genet*. 2012;8(5):e1002647.
22. Shpargel KB, Starmer J, Yee D, Pohlers M, Magnuson T. KDM6 demethylase independent loss of histone H3 lysine 27 trimethylation during early embryonic development. *PLoS Genet*. 2014;10(8):e1004507.
23. van Haaften G, Dalgliesh GL, Davies H, et al. Somatic mutations of the histone H3K27 demethylase gene UTX in human cancer. *Nat Genet*. 2009;41(5):521-523.
24. Varela I, Tarpey P, Raine K, et al. Exome sequencing identifies frequent mutation of the SWI/SNF complex gene PBRM1 in renal carcinoma [published correction appears in *Nature*. 2012;484(7392):130]. *Nature*. 2011;469(7331):539-542.
25. Gui Y, Guo G, Huang Y, et al. Frequent mutations of chromatin remodeling genes in transitional cell carcinoma of the bladder. *Nat Genet*. 2011;43(9):875-878.
26. Grasso CS, Wu YM, Robinson DR, et al. The mutational landscape of lethal castration-resistant prostate cancer. *Nature*. 2012;487(7406):239-243.
27. Jones DT, Jäger N, Kool M, et al. Dissecting the genomic complexity underlying medulloblastoma. *Nature*. 2012;488(7409):100-105.
28. Mar BG, Bullinger L, Basu E, et al. Sequencing histone-modifying enzymes identifies UTX mutations in acute lymphoblastic leukemia. *Leukemia*. 2012;26(8):1881-1883.
29. Robinson G, Parker M, Kranenburg TA, et al. Novel mutations target distinct subgroups of medulloblastoma. *Nature*. 2012;488(7409):43-48.
30. Wang L, Shilatifard A. UTX Mutations in Human Cancer. *Cancer Cell*. 2019;35(2):168-176.
31. Ribera J, Zamora L, Morgades M, et al; Spanish PETHEMA Group and the Spanish Society of Hematology. Copy number profiling of adult relapsed B-cell precursor acute lymphoblastic leukemia reveals potential leukemia progression mechanisms. *Genes Chromosomes Cancer*. 2017;56(11):810-820.
32. Stief SM, Hanneforth AL, Weser S, et al. Loss of KDM6A confers drug resistance in acute myeloid leukemia. *Leukemia*. 2020;34(1):50-62.
33. Zheng L, Xu L, Xu Q, et al. Utx loss causes myeloid transformation. *Leukemia*. 2018;32(6):1458-1465.
34. Gozdecka M, Meduri E, Mazan M, et al. UTX-mediated enhancer and chromatin remodeling suppresses myeloid leukemogenesis through noncatalytic inverse regulation of ETS and GATA programs. *Nat Genet*. 2018;50(6):883-894.
35. Ratajczak MZ, Suszynska M. Emerging Strategies to Enhance Homing and Engraftment of Hematopoietic Stem Cells. *Stem Cell Rev Rep*. 2016;12(1):121-128.
36. Ntziachristos P, Tsirigos A, Welstead GG, et al. Contrasting roles of histone 3 lysine 27 demethylases in acute lymphoblastic leukaemia. *Nature*. 2014;514(7523):513-517.
37. Nagamachi A, Matsui H, Asou H, et al. Haploinsufficiency of SAMD9L, an endosome fusion facilitator, causes myeloid malignancies in mice mimicking human diseases with monosomy 7. *Cancer Cell*. 2013;24(3):305-317.

38. Demarest RM, Ratti F, Capobianco AJ. It's T-ALL about Notch. *Oncogene*. 2008;27(38): 5082-5091.

39. Vervoort SJ, van Boxtel R, Coffer PJ. The role of SRY-related HMG box transcription factor 4 (SOX4) in tumorigenesis and metastasis: friend or foe? *Oncogene*. 2013;32(29): 3397-3409.

40. Glass C, Wilson M, Gonzalez R, Zhang Y, Perkins AS. The role of EVI1 in myeloid malignancies. *Blood Cells Mol Dis*. 2014;53(1-2): 67-76.

41. Sandoval S, Kraus C, Cho EC, et al. Sox4 cooperates with CREB in myeloid transformation. *Blood*. 2012;120(1):155-165.

42. Zhang H, Alberich-Jorda M, Amabile G, et al. Sox4 is a key oncogenic target in C/EBPα mutant acute myeloid leukemia. *Cancer Cell*. 2013;24(5):575-588.

43. Irvine DA, Copland M. Targeting hedgehog in hematologic malignancy. *Blood*. 2012; 119(10):2196-2204.

44. Bigas A, Waskow C. Blood stem cells: from beginning to end. *Development*. 2016; 143(19):3429-3433.

45. Wahlestedt M, Pronk CJ, Bryder D. Concise review: hematopoietic stem cell aging and the prospects for rejuvenation. *Stem Cells Transl Med*. 2015;4(2):186-194.

46. Liang Y, Van Zant G, Szilvassy SJ. Effects of aging on the homing and engraftment of murine hematopoietic stem and progenitor cells. *Blood*. 2005;106(4):1479-1487.

47. Sun D, Luo M, Jeong M, et al. Epigenomic profiling of young and aged HSCs reveals concerted changes during aging that reinforce self-renewal. *Cell Stem Cell*. 2014;14(5): 673-688.

48. Blank U, Karlsson S. TGF-β signaling in the control of hematopoietic stem cells. *Blood*. 2015;125(23):3542-3550.

49. Richardson C, Yan S, Vestal CG. Oxidative stress, bone marrow failure, and genome instability in hematopoietic stem cells. *Int J Mol Sci*. 2015;16(2):2366-2385.

50. Krivtsov AV, Twomey D, Feng Z, et al. Transformation from committed progenitor to leukaemia stem cell initiated by MLL-AF9. *Nature*. 2006;442(7104):818-822.

51. Ivanova NB, Dimos JT, Schaniel C, Hackney JA, Moore KA, Lemischka IR. A stem cell molecular signature. *Science*. 2002;298(5593): 601-604.

52. Chambers SM, Shaw CA, Gatza C, Fisk CJ, Donehower LA, Goodell MA. Aging hematopoietic stem cells decline in function and exhibit epigenetic dysregulation. *PLoS Biol*. 2007;5(8):e201.

53. Gekas C, Graf T. CD41 expression marks myeloid-biased adult hematopoietic stem cells and increases with age. *Blood*. 2013; 121(22):4463-4472.

54. Li T, Zhou ZW, Ju Z, Wang ZQ. DNA Damage Response in Hematopoietic Stem Cell Ageing. *Genomics Proteomics Bioinformatics*. 2016; 14(3):147-154.

55. Flach J, Bakker ST, Mohrin M, et al. Replication stress is a potent driver of functional decline in ageing haematopoietic stem cells. *Nature*. 2014;512(7513):198-202.

56. Zhang C, Hong Z, Ma W, et al. Drosophila UTX coordinates with p53 to regulate ku80 expression in response to DNA damage. *PLoS One*. 2013;8(11):e78652.

57. Gao J, Zou J, Li J, et al. Folate deficiency facilitates coordination of KDM6A with p53 in 1 response to DNA damage. *bioRxiv*. March 28, 2019. doi.org/10.1101/591768.

58. Purton LE, Scadden DT. Limiting factors in murine hematopoietic stem cell assays. *Cell Stem Cell*. 2007;1(3):263-270.

59. Yang YR, Bu FT, Yang Y, et al. LEFTY2 alleviates hepatic stellate cell activation and liver fibrosis by regulating the TGF-β1/Smad3 pathway. *Mol Immunol*. 2020;26: 31-39.

60. Chang H, Liu Y, Xue M, et al. Synergistic action of master transcription factors controls epithelial-to-mesenchymal transition. *Nucleic Acids Res*. 2016;44(6):2514-2527.

61. Oki S, Ohta T, Shioi G, et al. ChIP-Atlas: a data-mining suite powered by full integration of public ChIP-seq data. *EMBO Rep*. 2018; 19(12):e46255.

62. Placek K, Hu G, Cui K, et al. MLL4 prepares the enhancer landscape for Foxp3 induction via chromatin looping. *Nat Immunol*. 2017;18(9): 1035-1045.

63. Sun Y, Zhou B, Mao F, et al. HOXA9 Reprograms the Enhancer Landscape to Promote Leukemogenesis. *Cancer Cell*. 2018;34(4): 643-658.e5.

64. De S, Wurster AL, Precht P, Wood WH III, Becker KG, Pazin MJ. Dynamic BRG1 recruitment during T helper differentiation and activation reveals distal regulatory elements. *Mol Cell Biol*. 2011;31(7):1512-1527.

65. Shi J, Whyte WA, Zepeda-Mendoza CJ, et al. Role of SWI/SNF in acute leukemia maintenance and enhancer-mediated Myc regulation. *Genes Dev*. 2013;27(24): 2648-2662.

66. Bossen C, Murre CS, Chang AN, Mansson R, Rodewald HR, Murre C. The chromatin remodeler Brg1 activates enhancer repertoires to establish B cell identity and modulate cell growth. *Nat Immunol*. 2015;16(7): 775-784.

67. Hohmann AF, Martin LJ, Minder JL, et al. Sensitivity and engineered resistance of myeloid leukemia cells to BRD9 inhibition. *Nat Chem Biol*. 2016;12(9):672-679.

68. Li G, So AY-L, Sookram R, et al. Epigenetic silencing of miR-125b is required for normal B-cell development. *Blood*. 2018;131(17): 1920-1930.

69. Beerman I, Rossi DJ. Epigenetic Control of Stem Cell Potential during Homeostasis, Aging, and Disease. *Cell Stem Cell*. 2015;16(6): 613-625.

70. Goodell MA, Rando TA. Stem cells and healthy aging. *Science*. 2015;350(6265): 1199-1204.

71. Geiger H, de Haan G, Florian MC. The ageing haematopoietic stem cell compartment. *Nat Rev Immunol*. 2013;13(5):376-389.

72. Kramer A, Challen GA. The epigenetic basis of hematopoietic stem cell aging. *Semin Hematol*. 2017;54(1):19-24.

73. Wątroba M, Szukiewicz D. The role of sirtuins in aging and age-related diseases. *Adv Med Sci*. 2016;61(1):52-62.

74. Rimmelé P, Bigarella CL, Liang R, et al. Aging-like phenotype and defective lineage specification in SIRT1-deleted hematopoietic stem and progenitor cells. *Stem Cell Reports*. 2014; 3(1):44-59.

75. Brown K, Xie S, Qiu X, et al. SIRT3 reverses aging-associated degeneration. *Cell Rep*. 2013;3(2):319-327.

76. Wang H, Diao D, Shi Z, et al. SIRT6 Controls Hematopoietic Stem Cell Homeostasis through Epigenetic Regulation of Wnt Signaling. *Cell Stem Cell*. 2016;18(4):495-507.

77. Mohrin M, Shin J, Liu Y, et al. Stem cell aging. A mitochondrial UPR-mediated metabolic checkpoint regulates hematopoietic stem cell aging. *Science*. 2015;347(6228): 1374-1377.

78. Sen P, Shah PP, Nativio R, Berger SL. Epigenetic Mechanisms of Longevity and Aging. *Cell*. 2016;166(4):822-839.

79. Schulz WA, Lang A, Koch J, Greife A. The histone demethylase UTX/KDM6A in cancer: Progress and puzzles. *Int J Cancer*. 2019; 145(3):614-620.

80. Benyoucef A, Palii CG, Wang C, et al. UTX inhibition as selective epigenetic therapy against TAL1-driven T-cell acute lymphoblastic leukemia. *Genes Dev*. 2016;30(5): 508-521.

81. Van der Meulen J, Sanghvi V, Mavrakis K, et al. The H3K27me3 demethylase UTX is a gender-specific tumor suppressor in T-cell acute lymphoblastic leukemia. *Blood*. 2015;125(1): 13-21.

82. Mochizuki-Kashio M, Aoyama K, Sashida G, et al. Ezh2 loss in hematopoietic stem cells predisposes mice to develop heterogeneous malignancies in an Ezh1-dependent manner. *Blood*. 2015;126(10):1172-1183.

83. Sashida G, Wang C, Tomioka T, et al. The loss of Ezh2 drives the pathogenesis of myelofibrosis and sensitizes tumor-initiating cells to bromodomain inhibition. *J Exp Med*. 2016; 213(8):1459-1477.

84. Komai T, Inoue M, Okamura T, et al. Transforming Growth Factor-β and Interleukin-10 Synergistically Regulate Humoral Immunity *via* Modulating Metabolic Signals. *Front Immunol*. 2018;9:1364.

85. Zaiatz-Bittencourt V, Finlay DK, Gardiner CM. Canonical TGF-β Signaling Pathway Represses Human NK Cell Metabolism. *J Immunol*. 2018;200(12):3934-3941.

86. Liu L, Cheung TH, Charville GW, et al. Chromatin modifications as determinants of muscle stem cell quiescence and chronological aging. *Cell Rep*. 2013;4(1):189-204.

87. Faralli H, Wang C, Nakka K, et al. UTX demethylase activity is required for satellite cell-mediated muscle regeneration. *J Clin Invest*. 2016;126(4):1555-1565.

88. Schwörer S, Becker F, Feller C, et al. Epigenetic stress responses induce muscle stem-cell ageing by Hoxa9 developmental signals. *Nature*. 2016;540(7633):428-432.

89. Mertens J, Paquola ACM, Ku M, et al. Directly Reprogrammed Human Neurons Retain Aging-Associated Transcriptomic Signatures and Reveal Age-Related Nucleocytoplasmic Defects. *Cell Stem Cell*. 2015; 17(6):705-718.

90. Rinnerthaler M, Streubel MK, Bischof J, Richter K. Skin aging, gene expression and calcium. *Exp Gerontol*. 2015;68:59-65.

91. Mattson MP, Arumugam TV. Hallmarks of Brain Aging: Adaptive and Pathological Modification by Metabolic States. *Cell Metab*. 2018;27(6):1176-1199.

92. Andricovich J, Perkail S, Kai Y, Casasanta N, Peng W, Tzatsos A. Loss of KDM6A Activates Super-Enhancers to Induce Gender-Specific Squamous-like Pancreatic Cancer and Confers Sensitivity to BET Inhibitors. *Cancer Cell*. 2018;33(3): 512-526.e8.

93. Kaneko S, Li X. X chromosome protects against bladder cancer in females via a KDM6A-dependent epigenetic mechanism. *Sci Adv*. 2018;4(6):eaar5598.